Available online at www.sciencedirect.com
SCIENCE DIRECT
Journal of Sound and Vibration 296 (2006) 166–182
JOURNAL OF SOUND AND VIBRATION
www.elsevier.com/locate/jsvi

An approximate numerical method for the complex eigenproblem in systems characterised by a structural damping matrix

F. Cortés*, M.J. Elejabarrieta

Department of Mechanical Engineering, Mondragon Unibertsitatea, Loramendi 4, 20500, Mondragon, Spain

Received 19 October 2004; received in revised form 25 November 2005; accepted 21 February 2006
Available online 24 May 2006

Abstract

This paper presents an efficient numerical method that approximates the complex eigenvalues and eigenvectors in structural systems with viscoelastic damping materials, characterised by the complex structural damping matrix. This new method begins from the solution of the undamped system and approximates the complex eigenpair by finite increments using the eigenvector derivatives and the Rayleigh quotient. It is implemented in three different approaches: single-step, incremental and iterative schemes. The single-step technique is presented for systems with low and medium damping. From numerical examples, it can be verified that the errors committed by the approximate single-step technique with respect to the exact solutions, obtained by the IRAM method, are less than 0.2% when the loss factor of the material damping is lower than 1; this is a considerable improvement on other approximate methods. For higher damped systems an improvement to the previous approach is proposed by an incremental technique that keeps the accuracy without significantly increasing the computational time. The complex eigenproblem for materials whose mechanical properties are dependent on frequency is solved by a fast iterative approach, whose validity is proved using a four-parameter fractional derivative model.

1. Introduction

Surface damping treatments with viscoelastic materials are the passive damping techniques more commonly used for noise and vibration reduction [1–3]. For viscoelastic materials, the stress–strain relationship, $\sigma - \varepsilon$, can be written in a simple way considering the complex modulus E^* of the material [4,5], given by

$$\sigma = E^* \varepsilon, \tag{1}$$

where

$$E^* = (E' + \mathrm{i}E'') = E(1 + \mathrm{i}\eta), \tag{2}$$

*Corresponding author. Tel.: +34 943 794700; fax: +34 943 791536.
E-mail addresses: fcortes@eps.mondragon.edu (F. Cortés), mjelejabarrieta@eps.mondragon.edu (M.J. Elejabarrieta).

0022-460X/$ - see front matter © 2006 Elsevier Ltd. All rights reserved.
doi:10.1016/j.jsv.2006.02.016

Nomenclature

c	Nelson's scalar
$\mathbf{c}$	Fox and Kapoor's vector
E	elasticity modulus
E_r	modal strain energy
E^*	complex modulus
E'	storage modulus
E''	loss modulus
$\mathbf{f}$	vector used to compute the eigenderivatives
$\mathbf{F}$	nodal force vector
$\mathbf{H}$	structural damping matrix
i	imaginary unit, $\sqrt{-1}$
k	stiffness of the damper
$\mathbf{K}$	stiffness matrix
l	length of a finite element
L	length of the beam
m	mass
$\mathbf{M}$	mass matrix
n	size of the system
$q_{\max}$	maximum number of increments
$\mathbf{u}$	nodal displacement vector
$\mathbf{v}$	Nelson's vector
$\mathbf{w}$	Wang's vector
β	fractional parameter
δ	Wang's scalar
ε	strain
η	loss factor
κ	iteration error
λ	eigenvalue
Λ	diagonal matrix of truncated eigenvalues
ρ	volumetric density
σ	stress
τ	relaxation time
$\boldsymbol{\phi}$	eigenvector
$\boldsymbol{\phi}'_{r2}$	Zhang and Zerva's residual vector
$\boldsymbol{\Phi}$	complete modal matrix
$\bar{\boldsymbol{\Phi}}$	truncated modal matrix
$\boldsymbol{\Psi}$	Zhang and Zerva's matrix
ω	circular frequency

Subscripts and indices

0	static property
e	elastic property
i	finite element index
j	iteration index
k	vector component index
m	truncation order index
q	incremental index
r	modal index
v	viscoelastic property
∞	asymptotic property

Superscripts

*	complex number
T	transpose operator
H	hermitian or complex conjugate transpose operator
$(\bullet)'$	derivative of $(\bullet)$
-1	inverse operator
$+$	pseudoinverse operator

$E = E'$ and E'' are the storage and the loss modulus, respectively, and η is the loss factor, given by

$$\eta = \frac{E''}{E'}. \tag{3}$$

The frequency and temperature dependence of the storage modulus E and loss factor η distinguishes viscoelastic damping from other damping mechanisms [6]. Park [7] and Adhikari [8] discuss different approaches to the mathematical modelling of the behaviour of viscoelastic materials.

The analysis of complex geometry structures whose behaviour cannot be simplified to that of a beam or a plate needs to employ numerical techniques such as the finite element method (FEM) [9,10], which provides a matrix system given by

$$\mathbf{M}\ddot{\mathbf{u}} + (\mathbf{K} + \mathrm{i}\mathbf{H})\mathbf{u} = \mathbf{F}, \tag{4}$$

where $\mathbf{M}$, $\mathbf{K}$ and $\mathbf{H}$ are the mass, stiffness and structural damping matrices and $\mathbf{u}$ and $\mathbf{F}$ are the nodal displacement and force vectors, respectively. Normally, stationary (steady-state) systems are analysed in frequency-domain [11]. When the coefficients of the matrices are constant, Eq. (4) may be solved by the modal superposition technique, and the variable damping systems by the direct frequency method. The computational effort of the direct frequency method lies in solving the dynamic system equations, while in

the modal superposition method it lies in solving the complex eigenproblem. For large-scale systems, the complex eigenpair may be calculated by the classical methods of Lanczos [12] or Arnoldi [13], and more recently, the complex subspace iteration method [14]. However, these methods are not effective when the dynamical properties of viscoelastic materials are dependent on frequency, thus approximate methods are commonly used, e.g. the modal strain energy (MSE) (see Refs. [15–18] on the origins of this method) if the assumption of small damping is made, $\eta < 0.1$. This approximate method consists of solving the undamped eigenproblem and estimates the modal loss factor as follows:

$$\eta_r = \frac{\sum_{i=1}^{n} \eta_i E_{r,i}}{\sum_{i=1}^{n} E_{r,i}}, \tag{5}$$

where η_r is the loss factor estimated for the rth mode, η_i the material loss factor of the ith finite element, n the total number of elements in the system and $E_{r,i}$ the strain energy of the rth mode stored into the ith finite element, given by

$$E_{r,i} = \frac{1}{2} \boldsymbol{\phi}_r^{\mathrm{T}} \mathbf{K}_i \boldsymbol{\phi}_r, \tag{6}$$

where $\mathbf{K}_i$ is the elastic stiffness matrix of the ith element, $\boldsymbol{\phi}_r$ is the rth eigenvector of the undamped system or normal eigenvector and $(\bullet)^{\mathrm{T}}$ denotes the transpose vector. When the damping is variable with frequency, the iterative MSE modality consumes large computational time.

In short, an efficient method that solves the complex eigenproblem in structural systems with structural damping variable with frequency discretised by FEM is presented in this paper. The definition of the problem is given by

$$\left(-\lambda_r^*(\mathbf{M}_e + \mathbf{M}_v) + \mathbf{K}_e + \mathbf{K}_v(\omega) + \mathrm{i}\mathbf{H}(\omega)\right)\boldsymbol{\phi}_r^* = \mathbf{0}, \tag{7}$$

where $\mathbf{M}_e$ and $\mathbf{M}_v$ are the mass matrices of the elastic and viscoelastic materials, $\mathbf{K}_e$ is the stiffness matrix of the elastic materials, $\mathbf{K}_v(\omega)$ and $\mathbf{H}(\omega)$ are the real and imaginary parts of the complex stiffness matrix $\mathbf{K}_v^*(\omega)$ of the viscoelastic materials, $\mathbf{K}_v^*(\omega) = \mathbf{K}_v(\omega) + \mathrm{i}\mathbf{H}(\omega)$, which depends on circular frequency ω, and λ_r^* and $\boldsymbol{\phi}_r^*$ are the complex eigenvalue and eigenvector of the rth mode, respectively. The present method computes the complex eigenvalues and eigenvectors from the undamped solution using the eigenvector derivatives and the Rayleigh quotient. Consequently, the usual methods for computing the eigenpair derivatives in undamped systems with non-repeat eigenvalues are revised in Section 2. Next, the new approximate method that solves the complex eigenproblem where the complex modulus is constant with frequency is presented. The general case in which the damping is variable with frequency is analysed in Section 4. Some numerical applications are made in Section 5 to prove the efficacy of the method. The algorithms of the proposed procedures are compiled in the Appendix.

2. Theoretical background

2.1. Derivatives of eigenvalues and eigenvectors

The eigenvalue and eigenvector derivatives are commonly employed in structural optimisation and sensitivity analysis and in the study of stochastic systems. A revision of the methods to compute the eigenderivatives in undamped systems is made in Ref. [19]. These derivatives are calculated from the generalised eigenvalue problem, given by

$$(-\lambda_r \mathbf{M} + \mathbf{K})\boldsymbol{\phi}_r = \mathbf{0}, \tag{8}$$

where the n order mass $\mathbf{M}$ and stiffness $\mathbf{K}$ matrices are real, symmetric and positive-definite and λ_r and $\boldsymbol{\phi}_r$ are the corresponding rth eigenvalue and eigenvector. The latter may be arbitrarily normalised [11] as Eq. (9) indicates,

$$\boldsymbol{\phi}_r^{\mathrm{T}} \mathbf{M} \boldsymbol{\phi}_r = m_r, \tag{9}$$

where m_r is the modal mass. A frequently used technique is to normalise the eigenvectors with respect to the unit modal mass, in which $m_r = 1$. The eigenderivatives of the rth mode is obtained by differentiating Eq. (8),

$$-\lambda_r'\mathbf{M}\boldsymbol{\phi}_r + (-\lambda_r\mathbf{M}' + \mathbf{K}')\boldsymbol{\phi}_r + (-\lambda_r\mathbf{M} + \mathbf{K})\boldsymbol{\phi}_r' = \mathbf{0}, \tag{10}$$

where $(\bullet)'$ represents the derivative with respect to any parameter. Premultiplication by $\boldsymbol{\phi}_r^{\mathrm{T}}$ yields

$$-\lambda_r'\boldsymbol{\phi}_r^{\mathrm{T}}\mathbf{M}\boldsymbol{\phi}_r + \boldsymbol{\phi}_r^{\mathrm{T}}(-\lambda_r\mathbf{M}' + \mathbf{K}')\boldsymbol{\phi}_r + \boldsymbol{\phi}_r^{\mathrm{T}}(-\lambda_r\mathbf{M} + \mathbf{K})\boldsymbol{\phi}_r' = 0, \tag{11}$$

where the last term of the left-hand side of the equation is zero by virtue of Eq. (8) and of the symmetry of the matrices; then, the derivative of the rth eigenvalue becomes

$$\lambda_r' = \frac{\boldsymbol{\phi}_r^{\mathrm{T}}(-\lambda_r\mathbf{M}' + \mathbf{K}')\boldsymbol{\phi}_r}{\boldsymbol{\phi}_r^{\mathrm{T}}\mathbf{M}\boldsymbol{\phi}_r}. \tag{12}$$

If a vector $\mathbf{f}_r$ is defined as

$$\mathbf{f}_r = -(-\lambda_r\mathbf{M}' + \mathbf{K}' - \lambda_r'\mathbf{M})\boldsymbol{\phi}_r, \tag{13}$$

then a relationship between the eigenvector derivative $\boldsymbol{\phi}_r'$ and $\mathbf{f}_r$ can be deduced from Eq. (10),

$$(-\lambda_r\mathbf{M} + \mathbf{K})\boldsymbol{\phi}_r' = \mathbf{f}_r, \tag{14}$$

where $\boldsymbol{\phi}_r'$ cannot be solved directly because the matrix $(-\lambda_r\mathbf{M} + \mathbf{K})$ is singular. The immediate technique to solve Eq. (14) is to employ the pseudoinverse matrix $(\bullet)^+$,

$$\boldsymbol{\phi}_r' = (-\lambda_r\mathbf{M} + \mathbf{K})^+\mathbf{f}_r, \tag{15}$$

which can be calculated by the singular value decomposition (SVD) technique [20], which implies large computational efforts. Therefore in recent years several methods that facilitate the evaluation of the eigenvectors derivatives have been developed. The classical methods that calculate the derivative of non-repeating eigenvectors are the Nelson's [21] and Fox and Kapoor's [22] methods. From the latter some improvements have been developed for truncated systems such as the proposed by Wang [23] and by Zhang and Zerva [24].

2.2. The Nelson's method

The Nelson's method decomposes the derivative of the eigenvector $\boldsymbol{\phi}_r'$ in two terms: a particular solution $\mathbf{v}_r$ and another homogeneous $c_r\boldsymbol{\phi}_r$,

$$\boldsymbol{\phi}_r' = \mathbf{v}_r + c_r\boldsymbol{\phi}_r, \tag{16}$$

where the scalar c_r is obtained by previously differencing Eq. (9),

$$2\boldsymbol{\phi}_r^{\mathrm{T}}\mathbf{M}\boldsymbol{\phi}_r' + \boldsymbol{\phi}_r^{\mathrm{T}}\mathbf{M}'\boldsymbol{\phi}_r = 0, \tag{17}$$

and then Eqs. (16) and (17) may be combined to give

$$c_r = -\boldsymbol{\phi}_r^{\mathrm{T}}\mathbf{M}\mathbf{v}_r - \frac{1}{2}\boldsymbol{\phi}_r^{\mathrm{T}}\mathbf{M}'\boldsymbol{\phi}_r, \tag{18}$$

where the unit modal mass normalisation is assumed. The $\mathbf{v}_r$ vector is calculated by a pivoting procedure in Eq. (14). The advantage of this method is that for calculating the exact derivative of an eigenvector it is only necessary to know the corresponding eigenvalue and eigenvector. But the pivoting procedure requires large computational time and extensive memory space.

2.3. The Fox and Kapoor's method

This method, also known as the modal superposition method, involves that the eigenvector derivative $\boldsymbol{\phi}_r'$ can be derived by means of a linear combination of all the modes of the system,

$$\boldsymbol{\phi}_r' = \boldsymbol{\Phi}\,\mathbf{c}_r, \tag{19}$$

where the matrix $\mathbf{\Phi}$ represents the complete modal base. To calculate the $\mathbf{c}_r$ vector, Eq. (19) is substituted in Eq. (10) and it is premultiplied by any eigenvector $\boldsymbol{\phi}_k^{\mathrm{T}}$, $k \neq r$, then the $\mathbf{M}$ and $\mathbf{K}$-orthogonality property of the eigenvectors [11] provides

$$\mathbf{c}_r(k) = \begin{cases} \dfrac{\boldsymbol{\phi}_r^{\mathrm{T}}\mathbf{f}_r}{\lambda_k - \lambda_r}, & r \neq k, \\ -\frac{1}{2}\boldsymbol{\phi}_r^{\mathrm{T}}\mathbf{M}'\boldsymbol{\phi}_r, & r = k, \end{cases} \tag{20}$$

where $\mathbf{c}_r(k)$ is the kth element of the $\mathbf{c}_r$ vector. This method is simple to be implemented, but to obtain the exact solution, the complete modal base is required. The inconvenient of this method lies in large-scale systems, in which it is necessary to calculate more modes than those which are really necessary. Although enough accuracy can be obtained by truncating from a certain mode, there are variants that propose an improvement including a residual term, such as the Wang's and the Zhang and Zerva's methods.

2.4. The mode truncation improvements

Wang [23] proposes to compute only m eigenvalues, $m<n$, using an incomplete modal base $\overline{\mathbf{\Phi}}$. Wang suggests to add a residual static correction factor $\delta_r\mathbf{w}_r$ for reducing the error due to the modal truncation as follows:

$$\boldsymbol{\phi}_r' \approx \overline{\mathbf{\Phi}}\mathbf{c}_r + \delta_r\mathbf{w}_r, \tag{21}$$

where the $\mathbf{w}_r$ vector indicates the direction of the residual term and the δ_r scalar is the scale factor. To calculate $\mathbf{w}_r$, Eq. (21) is introduced into Eq. (14) employing $\delta_r = 1$, so that

$$(\mathbf{K} - \lambda_r\mathbf{M})\mathbf{w}_r = \mathbf{f}_r - (\mathbf{K} - \lambda_r\mathbf{M})\overline{\mathbf{\Phi}}\mathbf{c}_r \tag{22}$$

is obtained. The singularity of the term $(-\lambda_r\mathbf{M} + \mathbf{K})$ that multiplies $\mathbf{w}_r$ is avoided by assigning $\lambda_r = 0$ (static residual) and then the linear equations system

$$\mathbf{K}\mathbf{w}_r = \mathbf{f}_r - (\mathbf{K} - \lambda_r\mathbf{M})\overline{\mathbf{\Phi}}\mathbf{c}_r \tag{23}$$

can be solved for $\mathbf{w}_r$ and finally the scale factor δ_r yields

$$\delta_r = \frac{\mathbf{w}_r^{\mathrm{T}}\mathbf{f}_r}{\mathbf{w}_r^{\mathrm{T}}(\mathbf{K} - \lambda_r\mathbf{M})\mathbf{w}_r}. \tag{24}$$

Zhang and Zerva [24] propose an iterative method in which the static residual term $\boldsymbol{\phi}'_{r2,j}$, at jth iteration, is written as

$$\boldsymbol{\phi}'_{r2,j} = \mathbf{\Psi}\mathbf{f}_r + \lambda_r\mathbf{\Psi}\mathbf{M}\boldsymbol{\phi}'_{r2,j-1}, \tag{25}$$

where

$$\mathbf{\Psi} = \mathbf{K}^{-1} - \overline{\mathbf{\Phi}}\mathbf{\Lambda}^{-1}\overline{\mathbf{\Phi}}^{\mathrm{T}} \tag{26}$$

and

$$\mathbf{\Lambda} = \mathrm{diag}(\lambda_1, \lambda_2, \ldots, \lambda_m). \tag{27}$$

In contrast to the approximate Wang's method, the Zhang and Zerva's iterative modality converges to the exact solution.

3. The proposed method for constant damping

3.1. Introduction

The complex eigenproblem of Eq. (7) with constant damping is given by

$$\left(-\lambda_r^*\mathbf{M} + \mathbf{K}^*\right)\boldsymbol{\phi}_r^* = \mathbf{0}, \tag{28}$$

where $\mathbf{M}$ and $\mathbf{K}^*$ are the mass and the complex stiffness matrices of the complete system and λ_r^* and $\boldsymbol{\phi}_r^*$ are the rth complex eigenvalue and eigenvector, respectively. The proposed method begins from the undamped eigensolution given by

$$\left(-\lambda_{r,0}\mathbf{M}+\mathbf{K}\right)\boldsymbol{\phi}_{r,0}=\mathbf{0}, \tag{29}$$

where $\mathbf{K}$ is the elastic stiffness of the undamped system and $\lambda_{r,0}$ and $\boldsymbol{\phi}_{r,0}$ are the real undamped eigenpair. By considering the damping of the system, the stiffness matrix is increased a quantity $\Delta\mathbf{K}^*$, so that

$$\mathbf{K}^*=\mathbf{K}+\Delta\mathbf{K}^*, \tag{30}$$

where

$$\Delta\mathbf{K}^*=\mathrm{i}\mathbf{H}, \tag{31}$$

while $\mathbf{M}$ matrix remains constant. Thus, the eigenpair will be modified as follows:

$$\lambda_r^*=\lambda_{r,0}+\Delta\lambda_r^* \tag{32}$$

and

$$\boldsymbol{\phi}_r^*=\boldsymbol{\phi}_{r,0}+\Delta\boldsymbol{\phi}_r^*, \tag{33}$$

where $\Delta\lambda_r^*$ and $\Delta\boldsymbol{\phi}_r^*$ are the complex eigen-increments. The proposed method computes an approximation of the increments of the eigenpair by taking the derivatives of Eqs. (10) and (12) as linear finite increments, with $\boldsymbol{\Delta M}=\mathbf{0}$, given by

$$\left(-\Delta\lambda_r^*\mathbf{M}+\Delta\mathbf{K}\right)\boldsymbol{\phi}_{r,0}+(-\lambda_{r,0}\mathbf{M}+\mathbf{K})\Delta\boldsymbol{\phi}_r^*=\mathbf{0} \tag{34}$$

and

$$\Delta\lambda_r^*=\frac{\boldsymbol{\phi}_{r,0}^{\mathrm{T}}\Delta\mathbf{K}^*\boldsymbol{\phi}_{r,0}}{\boldsymbol{\phi}_{r,0}^{\mathrm{T}}\mathbf{M}\boldsymbol{\phi}_{r,0}}. \tag{35}$$

Different modalities may be employed to compute the finite increment $\Delta\boldsymbol{\phi}_r^*$: SVD, Nelson, Fox and Kapoor, Wang and Zhang and Zerva techniques. A three-stage study will be done:

(1) On the first stage, it is assumed that the eigenvectors of the damped system are the same than those of the undamped. It will be proved that this approach is equivalent to the MSE method, thus it is valid for small damping, where $\eta<0.1$;
(2) A single-step technique is applied to compute $\Delta\boldsymbol{\phi}_r^*$ and $\Delta\lambda_r^*$ on the second stage. The numerical applications of Section 5 will prove that this scheme is applicable in systems with medium damping, in which $\eta<0.5$. It will be also deduced that Fox and Kapoor and Nelson modalities are the most efficient for full and truncated problems, respectively;
(3) On the last stage $\Delta\boldsymbol{\phi}_r^*$ and $\Delta\lambda_r^*$ are evaluated by multiple steps through an incremental technique with the purpose to be applied in systems with higher damping, where $\eta>0.5$.

3.2. First stage: the eigenvectors do not change

For the first approach, it is assumed that the eigenvectors of the system are not influenced by damping, consequently they are the same as those of the undamped system, which implies that the increment of the eigenvector $\Delta\boldsymbol{\phi}_r^*$ is zero,

$$\Delta\boldsymbol{\phi}_r^*=\mathbf{0}. \tag{36}$$

Since the mass matrix does not change, $\mathbf{M}'=\mathbf{0}$, the derivative of any rth undamped eigenvalue taking Eq. (12) yields

$$\lambda_r'=\frac{\boldsymbol{\phi}_{r,0}^{\mathrm{T}}\mathbf{K}'\boldsymbol{\phi}_{r,0}}{\boldsymbol{\phi}_{r,0}^{\mathrm{T}}\mathbf{M}\boldsymbol{\phi}_{r,0}}. \tag{37}$$

Next, by means of linear approximation, the finite increment of the eigenvalue becomes

$$\Delta\lambda_r^* \approx \frac{\boldsymbol{\phi}_{r,0}^{\mathrm{T}}\Delta\mathbf{K}^*\boldsymbol{\phi}_{r,0}}{\boldsymbol{\phi}_{r,0}^{\mathrm{T}}\mathbf{M}\boldsymbol{\phi}_{r,0}} = \mathrm{i}\frac{\boldsymbol{\phi}_{r,0}^{\mathrm{T}}\mathbf{H}\boldsymbol{\phi}_{r,0}}{\boldsymbol{\phi}_{r,0}^{\mathrm{T}}\mathbf{M}\boldsymbol{\phi}_{r,0}}, \tag{38}$$

which implies that the eigenvalue of the damped system λ_r^* may be approximated according to

$$\lambda_r^* \approx \lambda_{r,0} + \Delta\lambda_r^* \approx \lambda_{r,0} + \mathrm{i}\frac{\boldsymbol{\phi}_{r,0}^{\mathrm{T}}\mathbf{H}\boldsymbol{\phi}_{r,0}}{\boldsymbol{\phi}_{r,0}^{\mathrm{T}}\mathbf{M}\boldsymbol{\phi}_{r,0}}, \tag{39}$$

wherefrom two important conclusions are drawn:

(1) The approximation of the eigenvalue of the damped system can be evaluated by the Rayleigh quotient using the undamped eigenvectors, as Eq. (42) shows. Indeed, the Rayleigh quotient is calculated for the rth undamped mode by

$$\lambda_{r,0} = \frac{\boldsymbol{\phi}_{r,0}^{\mathrm{T}}\mathbf{K}\boldsymbol{\phi}_{r,0}}{\boldsymbol{\phi}_{r,0}^{\mathrm{T}}\mathbf{M}\boldsymbol{\phi}_{r,0}}, \tag{40}$$

if it is substituted in Eq. (39), then the approximation of the complex eigenvalue is written as

$$\lambda_r^* = \frac{\boldsymbol{\phi}_{r,0}^{\mathrm{T}}\mathbf{K}\boldsymbol{\phi}_{r,0}}{\boldsymbol{\phi}_{r,0}^{\mathrm{T}}\mathbf{M}\boldsymbol{\phi}_{r,0}} + \mathrm{i}\frac{\boldsymbol{\phi}_{r,0}^{\mathrm{T}}\mathbf{H}\boldsymbol{\phi}_{r,0}}{\boldsymbol{\phi}_{r,0}^{\mathrm{T}}\mathbf{M}\boldsymbol{\phi}_{r,0}}, \tag{41}$$

wherefrom it is deduced that the approximation of λ_r^* is given by

$$\lambda_r^* = \frac{\boldsymbol{\phi}_{r,0}^{\mathrm{T}}(\mathbf{K}+\mathrm{i}\mathbf{H})\boldsymbol{\phi}_{r,0}}{\boldsymbol{\phi}_{r,0}^{\mathrm{T}}\mathbf{M}\boldsymbol{\phi}_{r,0}} = \frac{\boldsymbol{\phi}_{r,0}^{\mathrm{T}}\mathbf{K}^*\boldsymbol{\phi}_{r,0}}{\boldsymbol{\phi}_{r,0}^{\mathrm{T}}\mathbf{M}\boldsymbol{\phi}_{r,0}}, \tag{42}$$

which represents the Rayleigh quotient using the undamped eigenvectors.

(2) The modal loss factor is exactly the same as the one computed by the MSE method. Indeed, the modal loss factor η_r is defined by

$$\lambda_r^* = \lambda_r(1+\mathrm{i}\eta_r), \tag{43}$$

where λ_r is the real part of the complex eigenvalue. From Eqs. (39) and (40), the loss factor η_r yields

$$\eta_r = \frac{\boldsymbol{\phi}_r^{\mathrm{T}}\mathbf{H}\boldsymbol{\phi}_r}{\boldsymbol{\phi}_r^{\mathrm{T}}\mathbf{K}\boldsymbol{\phi}_r}, \tag{44}$$

which is exactly the same result that the provided by the MSE method. Thus the application domain of the first approach is restricted to small damping systems, where $\eta < 0.1$.

3.3. Second stage: single-step approach

An improvement is proposed by considering that the eigenvector varies due to the damping introduced into the system as Eq. (45) indicates,

$$\boldsymbol{\phi}_r^* = \boldsymbol{\phi}_{r,0} + \Delta\boldsymbol{\phi}_r^*, \tag{45}$$

and the eigenvalues are computed by means of the Rayleigh quotient,

$$\lambda_r^* = \frac{\boldsymbol{\phi}_r^{*\mathrm{T}}\mathbf{K}^*\boldsymbol{\phi}_r^*}{\boldsymbol{\phi}_r^{*\mathrm{T}}\mathbf{M}\boldsymbol{\phi}_r^*}. \tag{46}$$

The present method may be implemented in different possible modalities in function of the procedure used for the computation of the eigenvector increment $\Delta\boldsymbol{\phi}_r^*$: SVD, Nelson, Fox and Kapoor, Wang or Zhang and Zerva. The numerical applications of Section 5 will confirm that the present method is more efficient using Fox and Kapoor and Nelson varieties for full and truncated problems, which are summarised in Tables A1 and A2 of Appendix, respectively.

3.4. Third stage: incremental approach

An improvement to the previous approach is proposed for systems with higher damping using an incremental procedure. The simplest way to proceed is by dividing the total stiffness matrix variation $\Delta\mathbf{K}^* = \mathrm{i}\mathbf{H}$ in $q_{\max}$ equal increments $\Delta\mathbf{K}_q^*$, according to

$$\Delta\mathbf{K}_q^* = \frac{1}{q_{\max}}\mathrm{i}\mathbf{H}. \tag{47}$$

The numerical applications of Section 5 will confirm that in systems with non-proportional damping in which the loss factor is comprised between 0.5 and 1, two increments commit an error lesser than 0.1%. Tables A3 and A4 of Appendix show the algorithms for the proposed incremental method using the Fox and Kapoor and the Nelson modalities, respectively.

4. The proposed method for variable damping

Since the properties of viscoelastic materials are dependent on frequency, the eigensystem becomes a problem in which the coefficients of the matrices are dependent on eigenvalue as Eq. (48) indicates,

$$\left(-\lambda_r^*(\mathbf{M}_e + \mathbf{M}_v) + \mathbf{K}_e + \mathbf{K}_v(\omega_r) + \mathrm{i}\mathbf{H}(\omega_r)\right)\boldsymbol{\phi}_r^* = \mathbf{0}, \tag{48}$$

where the natural frequency ω_r of the rth mode is the real part of the square root of the complex eigenvalue λ_r^*,

$$\omega_r = \mathrm{Re}\left(\sqrt{\lambda_r^*}\right). \tag{49}$$

Here it is proposed to solve Eq. (48) by an iterative technique that begins by solving the problem with the static properties of the viscoelastic material. Once the complex stiffness matrix is evaluated at the computed eigenfrequency, the iterative method is applied in the way that is indicated in the scheme of Fig. 1. Tables A5 and A6 of Appendix show the algorithms for the present iterative method using the Fox and Kapoor and the Nelson modalities, respectively. The convergence criterion κ_j may be defined as Eq. (50) indicates,

$$\kappa_j = \max\left(\frac{\mathrm{Re}\left(\lambda_{r,j}^* - \lambda_{r,j-1}^*\right)}{\mathrm{Re}\left(\lambda_{r,j-1}^*\right)}, \frac{\mathrm{Im}\left(\lambda_{r,j}^* - \lambda_{r,j-1}^*\right)}{\mathrm{Im}\left(\lambda_{r,j-1}^*\right)}\right), \tag{50}$$

in this way it is assured that the eigenvalues converge in the imaginary and real part as well. In comparison with the iterative MSE, the present method solves only once the undamped eigenproblem, while the MSE must do it once for each iteration, which increases the computational cost.

5. Numerical applications

5.1. Problem definition

The complex modes of the axial vibration problem of the damped beam represented in Fig. 2 will be solved. The beam is clamped on the left-hand side, and on the right-hand side a viscoelastic spring actuates, which is modelled by complex stiffness. The material of the beam is considered elastic in all applications with except for the last one, in which a complex modulus will be considered.

The beam is discretised in n standard truss finite elements. The $\mathbf{M}_i$ mass and $\mathbf{K}_i$ stiffness matrices of the ith finite element are given by

$$\mathbf{M}_i = \frac{\rho S l_i}{6}\begin{bmatrix} 2 & 1 \\ 1 & 2 \end{bmatrix} \tag{51}$$

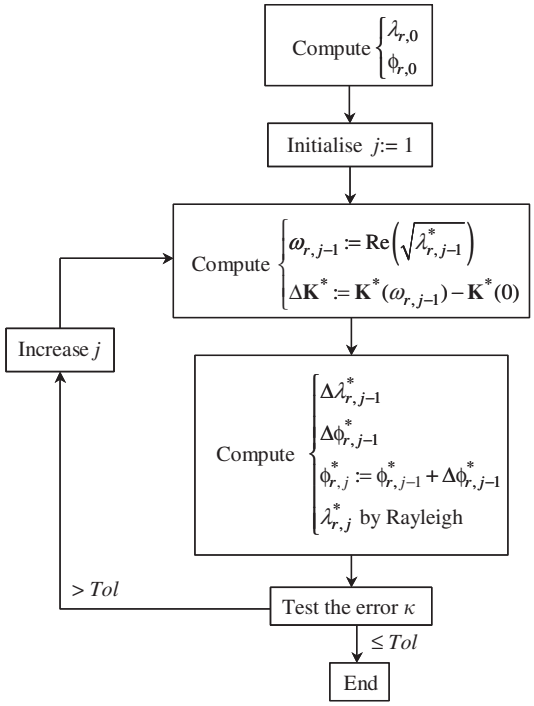

Fig. 1. Iterative scheme for variable damping.

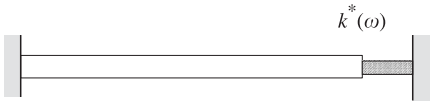

Fig. 2. Beam with viscoelastic spring.

and

$$\mathbf{K}_i = \frac{ES}{l_i}\begin{bmatrix} 1 & -1 \\ -1 & 1 \end{bmatrix}, \tag{52}$$

respectively, where ρ and E are the density and the elastic modulus of the material of the beam, S is the cross-sectional area and l_i is the length of the ith finite element. For the numerical examples, n equal finite elements will be chosen, that is $l_i = L/n$, where L is the length of the beam. The numerical values $\rho = 7860\,\mathrm{kg/m^3}$, $E = 210 \times 10^9\,\mathrm{Pa}$, $S = 100 \times 10^{-6}\,\mathrm{m^2}$ and $L = 1\,\mathrm{m}$ are taken. The computations were carried out in double arithmetic precision (16 digits) on a personal computer using Matlab [25] under windows environment.

The exact solution will be evaluated by the Implicit Restarted Arnoldi Method (IRAM) [26] implemented in Matlab ('eigs' command) and in the free software ARPACK [27] that is specially conceived for solving large-scale systems. The numerical applications are divided in three groups, which will prove the effectiveness and accuracy of the single-step, incremental and iterative approach for systems with low-medium, high and variable damping, respectively. The derivatives used by the present method are computed by different modalities: the SVD, Nelson's and Fox and Kapoor's techniques for full solutions and also by the Wang's and by the Zhang and Zerva's methods in truncated systems.

5.2. Numerical applications for the single-step approach

The CPU time is evaluated considering that the complex stiffness of the spring $k^* = k_e(1 + \mathrm{i}\eta)$ is constant, $k_e = 210 \times 10^5\,\mathrm{N/m}$ and $\eta = 1$. Tables 1 and 2 show the computational time, in seconds, employed to solve

Table 1
CPU time (s) in function of the DOF of the system (full solution)

DOF		50	100	150	200	250	300
IRAM		0.141	0.468	1.360	3.297	6.484	11.41
T_0		0.015	0.032	0.063	0.188	0.234	0.484
Present	SVD	0.374	3.829	18.03	64.31	190.1	392.5
	Nelson	0.046	0.265	1.250	3.046	6.250	12.48
	Fox and Kapoor	0.030	0.094	0.219	0.516	0.796	1.406

Table 2
CPU time (s) in function of the DOF of the system (truncated solution)

DOF		50	100	150	200	250	300	1000
IRAM		0.063	0.093	0.204	0.313	0.469	0.766	16.14
T_0		0.125	0.141	0.203	0.250	0.329	0.422	7.594
Present	SVD	0.203	0.516	1.374	3.312	7.547	12.89	490.1
	Nelson	0.125	0.155	0.249	0.392	0.588	0.844	12.81
	Fox and Kapoor	0.125	0.141	0.203	0.265	0.345	0.437	7.844
	Wang	0.125	0.172	0.249	0.391	0.563	0.782	13.06
	Zhang and Zerva	0.140	0.204	0.469	0.797	1.423	2.219	62.87

Table 3
Error on modal properties in function of η (full solution)

η	0.001	0.1	0.5	1	2
ω_1(%)	<0.001	<0.001	0.005	0.069	0.894
η_1(%)	<0.001	<0.001	0.012	0.186	2.766
MAC_1	≈ 1	≈ 1	0.99999	0.99987	0.99790

the full and truncated (10 modes) problems, respectively, in a system from 50 to 1000 finite elements, that in this case is equal to the DOF number of the system. In the first row of the tables the time needed to obtain the exact solution by IRAM is showed. In the second one the T_0 time is included, which represents the necessary time for solving the undamped problem. The rest of the rows contain the time needed by the proposed method using different modalities.

It can be pointed out that the proposed method using the Fox and Kapoor modality is faster than the exact IRAM method, even if the latter is conceived for large scale systems. The Nelson modality is the fastest between the methods for truncated solutions. Consequently, from now on these two modalities are exclusively taken into account for the next applications.

The application range of the present scheme is evaluated using a system of 100 DOF. The accuracy is estimated in function of the level of the loss factor of the damper, which is taken over the interval $0.001 \leqslant \eta \leqslant 2$ (from the level of some metals to that of some elastomers). The accuracy for full and truncated (10 modes) solutions is represented in Table 3 and in Table 4, respectively. The modal properties for exact solution, computed by the IRAM method, are compared with these of the present method using the Fox and Kapoor and the Nelson modalities. Only the solutions of the first mode are compared, because this is the mode that has presented the highest error. The two first rows indicate in percentage the absolute value of the difference on the natural frequency ω_1 and on the modal loss factor η_1, respectively, between IRAM and present methods. In the third row the eigenvectors $\boldsymbol{\phi}_1^*$ are compared through the Modal Assurance Criterion (MAC) [11] method, which helps to evaluate the degree of correlation between two modal vectors $\boldsymbol{\phi}_i^*$ and $\boldsymbol{\phi}_j^*$. It

Table 4
Error on modal properties in function of η (truncated solution)

η		0.001	0.1	0.5	1	2
Present	$\omega_1(\%)$	<0.001	<0.001	0.005	0.069	0.894
—	$\eta_1(\%)$	<0.001	<0.001	0.012	0.186	2.766
Nelson	MAC_1	≈ 1	≈ 1	0.99999	0.99987	0.99790
Present	$\omega_1(\%)$	<0.001	0.003	0.074	0.213	0.065
—	$\eta_1(\%)$	<0.001	0.014	0.335	1.200	2.772
Fox and Kapoor	MAC_1	≈ 1	0.99999	0.99999	0.99986	0.89382

Table 5
Improvement provided by incremental method (full solution)

Mode	Present—Fox and Kapoor single-step approach			Present—Fox and Kapoor 2 increments approach		
	$\omega_r(\%)$	$\eta_r(\%)$	MAC_r	$\omega_r(\%)$	$\eta_r(\%)$	MAC_r
1	0.069	0.186	0.99987	0.017	0.061	0.99997
2	0.005	0.031	0.99987	0.001	0.013	0.99997
3	<0.001	0.002	0.99999	<0.001	<0.001	≈ 1

uniquely identifies a real scale between zero and one and it is defined by

$$\mathrm{MAC} = \frac{\left|\boldsymbol{\phi}_i^{*\mathrm{H}}\boldsymbol{\phi}_j^{*}\right|^2}{\left(\boldsymbol{\phi}_i^{*\mathrm{H}}\boldsymbol{\phi}_i^{*}\right)\cdot\left(\boldsymbol{\phi}_j^{*\mathrm{H}}\boldsymbol{\phi}_j^{*}\right)}, \tag{53}$$

where $(\bullet)^{\mathrm{H}}$ denotes the complex conjugate transpose vector.

For low and medium damping, $\eta<0.5$, the Fox and Kapoor modality commits errors on modal properties minor than 0.1%, but losses precision when all modes are not employed whereas the Nelson modality is not influenced by the truncation effect, because it uses exclusively the eigenpair under consideration. Therefore, the present method is proposed with Fox and Kapoor derivatives for full problems and with Nelson when few modes are required. In both cases the accuracy may be not enough for higher damped systems, where $\eta>0.5$, for which the incremental approach is proposed.

5.3. Numerical applications for the incremental approach

For improving the accuracy of the present method in higher damped systems, the incremental approach will be evaluated using a 100 DOF system, in which $\eta = 1$. Tables 5 and 6 compare the accuracy of the single-step using the Fox and Kapoor and the Nelson modalities with the incremental scheme. For the Nelson case only 3 modes are computed.

From these two tables it can be pointed out that the accuracy has been increased more than 50% when 2 steps are used.

5.4. Numerical applications for variable damping

5.4.1. Numerical example 1

The frequency dependence of the complex stiffness $k^*(\omega)$ of the damper will be modelled by a four-parameter fractional derivative model [28], given by

$$k^*(\omega) = \frac{k_0 + k_\infty(\mathrm{i}\tau\omega)^\beta}{1 + (\mathrm{i}\tau\omega)^\beta}, \tag{54}$$

Table 6
Improvement provided by incremental method (truncated solution)

Mode	Present—Nelson single-step approach			Present—Nelson 2 increments approach		
	$\omega_r(\%)$	$\eta_r(\%)$	MAC_r	$\omega_r(\%)$	$\eta_r(\%)$	MAC_r
1	0.069	0.186	0.99987	0.017	0.064	0.99997
2	0.005	0.031	0.99987	0.001	0.011	0.99997
3	<0.001	0.002	0.99999	<0.001	<0.001	≈ 1

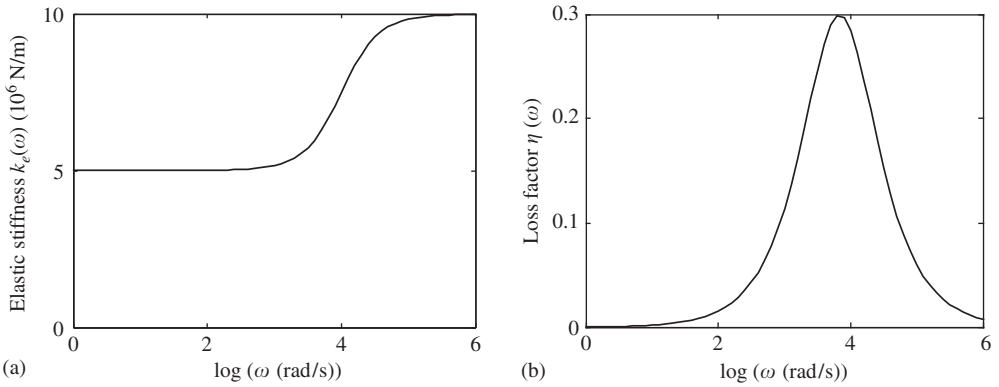

Fig. 3. Properties of the spring: (a) elastic stiffness $k_e(\omega)$ and (b) loss factor $\eta(\omega)$.

Table 7
Modal properties of the 3 DOF system with variable damping

	Mode 1		Mode 2		Mode 3	
$\lambda_r^* = \lambda_r(1+i\eta_r)$ (10^9 rad^2/s^2)	0.0859 + i 0.0050		0.7561 + i 0.0058		2.4408 + i 0.0074	
$\omega_r(10^3$ rad/s)	9.273		27.50		49.40	
η_r	0.0581		0.0077		0.0030	
$\boldsymbol{\phi}_r^*$ (modulus | phase)	0.8668	$\lvert 0.927^\circ$	1.9537	$\lvert 0.001^\circ$	1.2539	$\lvert -0.215^\circ$
	1.4413	$\lvert 0.290^\circ$	0.1252	$\lvert 9.393^\circ$	2.2207	$\lvert -0.077^\circ$
	1.5302	$\lvert -1.068^\circ$	1.9461	$\lvert -0.075^\circ$	2.6789	$\lvert 0.191^\circ$

where k_0 and k_∞ represent the elastic and asymptotic stiffness, respectively, τ is the relaxation time that is related with the frequency at which the loss factor reaches its maximum value and β is the fractional parameter, $0<\beta<1$, which is related with the maximum value of the loss factor. Fig. 3 represents the evolution of the elastic stiffness $k_e(\omega)$ and the loss factor $\eta(\omega)$ in function of the frequency ω (in rad/s) when $k_0 = 5\times10^6$ N/m, $k_\infty = 10\times10^6$ N/m, $\tau = 10^{-4}$ s and $\beta = 0.9$.

The bar, whose elastic modulus is $E = 210\times10^9$ Pa, is still elastic, and a 3 DOF system is under study. The exact solution is given by the IRAM method using an iterative technique, which provides the solution of the three modes showed in Table 7: the eigenvalue λ_r^*, the real natural frequency ω_r, the modal loss factor η_r and the eigenvector $\boldsymbol{\phi}_r$, normalised with respect to the unit modal mass.

Table 8 shows the error committed by the proposed iterative approach and by the iterative MSE, both compared with the exact solution that was illustrated in Table 7.

From Table 8 it should be noted that the differences are more pronounced for the first mode, which is the highest damped mode. It can also be pointed out that the present method is more accurate than the iterative

Table 8
Error on modal properties by iterative methods

Mode	Present			MSE		
	$\omega_r(\%)$	$\eta_r(\%)$	MAC_r	$\omega_r(\%)$	$\eta_r(\%)$	MAC_r
1	<0.001	<0.001	≈ 1	0.056	0.135	0.99957
2	<0.001	0.003	≈ 1	0.001	0.003	0.99954
3	<0.001	<0.001	≈ 1	0.001	0.002	0.99984

Table 9
Modal properties of the 3 DOF system with variable damping (fully damping matrix)

	Mode 1		Mode 2		Mode 3	
$\lambda_r^* = \lambda_r(1+\mathrm{i}\eta_r)$ $(10^9\,\mathrm{rad}^2/\mathrm{s}^2)$	$0.0859+\mathrm{i}\,0.0187$		$0.7561+\mathrm{i}\,0.1501$		$2.4408+\mathrm{i}\,0.4818$	
$\omega_r(10^3\,\mathrm{rad/s})$	9.320		27.63		49.64	
η_r	0.2179		0.1986		0.1974	
$\boldsymbol{\phi}_r^*$ (modulus | phase)	0.8674	$\lvert 0.2749^\circ$	1.9537	$\lvert 0.000^\circ$	1.2547	$\lvert -0.176^\circ$
	1.4416	$\lvert 0.0860^\circ$	0.1229	$\lvert -1.710^\circ$	2.2212	$\lvert -0.063^\circ$
	1.5284	$\lvert -0.3174^\circ$	1.9462	$\lvert -0.013^\circ$	2.6775	$\lvert 0.156^\circ$

Table 10
Error on modal properties by iterative methods (fully damping matrix)

Mode	Present			MSE		
	$\omega_r(\%)$	$\eta_r(\%)$	MAC_r	$\omega_r(\%)$	$\eta_r(\%)$	MAC_r
1	0.003	0.011	0.99991	0.005	0.020	0.99972
2	<0.001	0.002	0.99998	<0.001	<0.001	0.99960
3	<0.001	0.002	0.99999	<0.001	0.001	0.99986

MSE. Besides, the former solves the undamped problem only once, while the latter must do it once in each iteration, which increases the computational cost.

5.4.2. Numerical example 2

The imaginary part of the stiffness matrix of the previous system contains only a few non-zero entries. The next example will consider that the material of the beam is also viscoelastic and it will be modelled by a complex modulus $E^* = E(1+\mathrm{i}\eta)$ constant in frequency, where $E = 210\times10^9\,\mathrm{Pa}$ and $\eta = 0.2$. The same fractional model of the previous section is taken for the complex stiffness $k^*(\omega)$ of the damper. Indeed, while the previous examples have been able to examine the influence of the truncation effect and of the level of the loss factor on the accuracy, the aim of this example is to prove the new method in a fully populated damping matrix. Table 9 shows the exact solution by IRAM and Table 10 illustrates the accuracy of the proposed method.

It can be remarked that the conclusions of the previous example are also valid in this case in which the damping matrix is fully populated.

6. Concluding remarks

An efficient numerical method that approximates the complex eigenvalues and eigenvectors in systems with viscoelastic damping materials has been developed and implemented in a finite element environment. This new

method begins from the solution of the undamped system and approximates the complex eigenpair by finite increments using the eigenvector derivatives and the Rayleigh quotient. From the numerical examples it has been proved that the Fox and Kapoor and the Nelson derivatives are the most efficient in full and truncated problems, respectively. The numerical applications also have proved that the proposed numerical method is an effective way for computing the complex eigenvalues and eigenvectors in systems with structural damping matrix. In effect,

(a) it was verified that errors committed by the approximate single-step technique with respect to the exact solution are less than 0.1% when the loss factor of the material damping is lower than 0.5. This improves considerably the precision of other approximate methods;
(b) for higher damped systems, the wished precision can be achieved with the incremental technique using the appropriate number of increments without significantly increasing the computational time. The numerical examples have confirmed that two increments commit an error less than 0.1% when the loss factor is comprised between 0.5 and 1;
(c) in systems with variable damping, the iterative modality of the present method solves once the eigenproblem of undamped problem, so the convergence time is accelerated in comparison to other approximate methods. The only restriction of the method is that the real part of the eigenvalues must not change substantially.

Acknowledgements

The authors would like to thank Unai Galfarsoro and Iñaki Hurtado from Mondragon Unibertsitatea for the help provided in English grammar.

Appendix. Algorithms

See Tables A1–A6.

At each iteration, the $\kappa_{r,j}$ error used to compare with the convergence tolerance may be defined arbitrarily, e.g. as it is indicated as follows:

$$\kappa_{r,j} = \max\left(\frac{\mathrm{Re}\left(\lambda^*_{r,j} - \lambda^*_{r,j-1}\right)}{\mathrm{Re}\left(\lambda^*_{r,j-1}\right)}, \frac{\mathrm{Im}\left(\lambda^*_{r,j} - \lambda^*_{r,j-1}\right)}{\mathrm{Im}\left(\lambda^*_{r,j-1}\right)}\right).$$

Table A1
Algorithm for the single-step method using the Fox and Kapoor derivatives

1. Solve the undamped problem $(-\lambda_{r,0}\mathbf{M} + \mathbf{K})\boldsymbol{\phi}_{r,0} = \mathbf{0}$, where $\boldsymbol{\phi}^{\mathrm{T}}_{r,0}\mathbf{M}\boldsymbol{\phi}_{r,0} = 1$.
2. Compute $\mathbf{f}_{r,0} := -\mathbf{H}\boldsymbol{\phi}_{r,0}$.
3. Construct the $\mathbf{c}_r$ vector of dimension n;
   for k from 1 to m, where $m \leqslant n$, do
   if $k \neq r$ then $\mathbf{c}_r(k) := \dfrac{\boldsymbol{\phi}^{\mathrm{T}}_{k,0}\mathbf{f}_r}{\lambda_{k,0} - \lambda_{r,0}}$,
   if $k \neq r$ then $\mathbf{c}_r(k) := 0$.
4. Compute $\boldsymbol{\phi}^*_r := \boldsymbol{\phi}_{r,0} + \mathrm{i}\boldsymbol{\Phi}_0\mathbf{c}_r$.
5. Normalize $\boldsymbol{\phi}^*_r := \dfrac{\boldsymbol{\phi}^*_r}{\sqrt{\boldsymbol{\phi}^{*\mathrm{T}}_r\mathbf{M}\boldsymbol{\phi}^*_r}}$.
6. Compute $\lambda^*_r := \boldsymbol{\phi}^{*\mathrm{T}}_r\mathbf{K}^*\boldsymbol{\phi}^*_r$.

Table A2
Algorithm for the single-step method using the Nelson derivatives

1. Solve the undamped problem $(-\lambda_{r,0}\mathbf{M}+\mathbf{K})\boldsymbol{\phi}_{r,0}=\mathbf{0}$, where $\boldsymbol{\phi}_{r,0}^{\mathrm{T}}\mathbf{M}\boldsymbol{\phi}_{r,0}=1$.
2. Compute $\Delta\lambda_r := \boldsymbol{\phi}_{k,0}^{\mathrm{T}}\mathbf{H}\boldsymbol{\phi}_{r,0}$.
3. Compute $\mathbf{f}_r := -(-\Delta\lambda_r\mathbf{M}+\mathbf{H})\boldsymbol{\phi}_{r,0}$.
4. Compute $\mathbf{G}_r := -\lambda_{r,0}\mathbf{M}+\mathbf{K}$.
5. Find the k position of the element with largest absolute value in $\boldsymbol{\phi}_{r,0}$ vector.
6. Construct $\bar{\mathbf{G}}_r$ by zeroing out the k row and column of $\mathbf{G}_r$ and setting the k diagonal element to 1.
7. Construct $\bar{\mathbf{f}}_r$ by zeroing out the kth element of $\mathbf{f}_r$.
8. Solve $\mathbf{v}_r$ from the linear equation system $\bar{\mathbf{G}}_r\mathbf{v}_r=\bar{\mathbf{f}}_r$.
9. Compute $c_r := -\boldsymbol{\phi}_{r,0}^{\mathrm{T}}\mathbf{M}\mathbf{v}_r$.
10. Compute $\boldsymbol{\phi}_r^* := \boldsymbol{\phi}_{r,0}+\mathrm{i}(\mathbf{v}_r+c_r\boldsymbol{\phi}_{r,0})$.
11. Normalize $\boldsymbol{\phi}_r^* := \dfrac{\boldsymbol{\phi}_r^*}{\sqrt{\boldsymbol{\phi}_r^{*\mathrm{T}}\mathbf{M}\boldsymbol{\phi}_r^*}}$.
12. Compute $\lambda_r^* := \boldsymbol{\phi}_r^{*\mathrm{T}}\mathbf{K}^*\boldsymbol{\phi}_r^*$.

Table A3
Algorithm for the incremental method using the Fox and Kapoor derivatives

1. Solve the undamped problem $(-\lambda_{r,0}\mathbf{M}+\mathbf{K})\boldsymbol{\phi}_{r,0}=\mathbf{0}$, where $\boldsymbol{\phi}_{r,0}^{\mathrm{T}}\mathbf{M}\boldsymbol{\phi}_{r,0}=1$.
2. Compute $\mathbf{h}^* := \frac{1}{q_{\max}}\mathrm{i}\mathbf{H}$.
3. For q from 1 to $q_{\max}$ do
    4. For r from 1 to m do
        5. Compute $\mathbf{f}_{r,q}^* := -\mathbf{h}^*\boldsymbol{\phi}_{r,q-1}^*$.
        6. Construct the $\mathbf{c}_{r,q}^*$ vector of dimension n;
            for k from 1 to m, where $m\leqslant n$, do
                if $k\neq r$ then $\mathbf{c}_{r,q}^*(k) := \dfrac{\boldsymbol{\phi}_{k,q-1}^{*\mathrm{T}}\mathbf{f}_{r,q}^*}{\lambda_{k,q-1}^*-\lambda_{r,q-1}^*}$,
                if $k=r$ then $\mathbf{c}_{r,q}^*(k) := 0$.
        7. Compute $\Delta\boldsymbol{\phi}_{r,q}^* := \boldsymbol{\Phi}_{q-1}^*\mathbf{c}_{r,q}^*$.
    8. Normalise $\boldsymbol{\phi}_{r,q}^* := \dfrac{\boldsymbol{\phi}_{r,q}^*}{\sqrt{\boldsymbol{\phi}_{r,q}^{*\mathrm{T}}\mathbf{M}\boldsymbol{\phi}_{r,q}^*}}$.
    9. Compute $\lambda_{r,q}^* := \boldsymbol{\phi}_{r,q}^{*\mathrm{T}}(\mathbf{K}+q\,\mathbf{h}^*)\boldsymbol{\phi}_{r,q}^*$.

Table A4
Algorithm for the incremental method using the Nelson derivatives

1. Solve the undamped problem $(-\lambda_{r,0}\mathbf{M}+\mathbf{K})\boldsymbol{\phi}_{r,0}=\mathbf{0}$, where $\boldsymbol{\phi}_{r,0}^{\mathrm{T}}\mathbf{M}\boldsymbol{\phi}_{r,0}=1$.
2. Compute $\mathbf{h}^* := \frac{1}{q_{\max}}\mathrm{i}\mathbf{H}$.
3. For q from 1 to $q_{\max}$ do
    4. Compute $\Delta\lambda_{r,q-1}^* := \boldsymbol{\phi}_{r,q-1}^{*\mathrm{T}}\,\mathbf{h}^*\,\boldsymbol{\phi}_{r,q-1}^*$.
    5. Compute $\mathbf{f}_{r,q}^* := -(-\Delta\lambda_{r,q}^*\mathbf{M}+\mathbf{h}^*)\boldsymbol{\phi}_{r,q-1}^*$.
    6. Compute $\mathbf{G}_{r,q}^* := -\lambda_{r,q-1}^*\mathbf{M}+(q-1)\mathbf{h}^*$.
    7. Find the k position of the element with largest absolute value in $\boldsymbol{\phi}_{r,q}^*$ vector.
    8. Construct $\bar{\mathbf{G}}_{r,q}^*$ by zeroing out the k row and column of $\mathbf{G}_{r,q}^*$ and setting the k diagonal element to 1.
    9. Construct $\bar{\mathbf{f}}_{r,q}^*$ by zeroing out the kth element of $\mathbf{f}_{r,q}^*$.
    10. Solve $\mathbf{v}_{r,q}^*$ from the linear equation system $\bar{\mathbf{G}}_{r,q}^*\mathbf{v}_{r,q}^*=\bar{\mathbf{f}}_{r,q}^*$.
    11. Compute $c_{r,q}^* := -\boldsymbol{\phi}_{r,q-1}^{*\mathrm{T}}\mathbf{M}\mathbf{v}_{r,q}^*$.
    12. Compute $\boldsymbol{\phi}_{r,q}^* := \boldsymbol{\phi}_{r,q-1}^*+(\mathbf{v}_{r,q}^*+c_{r,q}^*\boldsymbol{\phi}_{r,q-1}^*)$.
    13. Normalize $\boldsymbol{\phi}_{r,q}^* := \dfrac{\boldsymbol{\phi}_{r,q}^*}{\sqrt{\boldsymbol{\phi}_{r,q}^{*\mathrm{T}}\mathbf{M}\boldsymbol{\phi}_{r,q}^*}}$.
    14. Compute $\lambda_{r,q}^* := \boldsymbol{\phi}_{r,q}^{*\mathrm{T}}(\mathbf{K}+q\,\mathbf{h}^*)\boldsymbol{\phi}_{r,q}^*$.

Table A5
Algorithm for the iterative method using the Fox and Kapoor derivatives

1. Solve the undamped problem $\left(-\lambda_{r,0}\mathbf{M}+\mathbf{K}_e+\mathbf{K}_v^*(0)\right)\boldsymbol{\phi}_{r,0}=\mathbf{0}$, where $\boldsymbol{\phi}_{r,0}^{\mathrm{T}}\mathbf{M}\boldsymbol{\phi}_{r,0}=1$.
2. Initialize $j:=1$, define the convergence tolerance *Tol* and the maximum number of iterations $j_{\max}$.
3. Repeat
   4. Compute the real eigenfrequency $\omega_{r,j-1}$.
   5. Compute $\Delta\mathbf{K}_{r,j-1}^*=\mathbf{K}_v^*(\omega_{r,j-1})-\mathbf{K}_v^*(0)$.
   6. Compute $\mathbf{f}_{r,j}^*:=-\Delta\mathbf{K}_{r,j-1}^*\boldsymbol{\phi}_{r,0}$.
   7. Construct the $\mathbf{c}_{r,j}^*$ vector of dimension n;
      for k from 1 to m, where $m\leqslant n$, do
      if $k\neq r$ then $\mathbf{c}_{r,q}^*(k):=\dfrac{\boldsymbol{\phi}_{k,0}^{\mathrm{T}}\mathbf{f}_{r,j}^*}{\lambda_{k,0}-\lambda_{r,0}}$,
      if $k=r$ then $\mathbf{c}_{r,j}^*(k):=0$.
   8. Compute $\boldsymbol{\phi}_{r,j}^*:=\boldsymbol{\phi}_{r,0}+\boldsymbol{\Phi}_0\mathbf{c}_{r,j}^*$.
   9. Normalize $\boldsymbol{\phi}_{r,j}^*:=\dfrac{\boldsymbol{\phi}_{r,j}^*}{\sqrt{\boldsymbol{\phi}_{r,j}^{*\mathrm{T}}\mathbf{M}\boldsymbol{\phi}_{r,j}^*}}$.
   10. Compute $\lambda_{r,j}^*:=\boldsymbol{\phi}_{r,j}^{*\mathrm{T}}\mathbf{K}^*(\omega_{r,j-1})\boldsymbol{\phi}_{r,j}^*$.
   11. Compute the error $\kappa_{r,j}$ and increase $j:=j+1$.

Until $\kappa_{r,j}\leqslant Tol$ or $j>j_{\max}$.

Table A6
Algorithm for the iterative method using the Nelson derivatives

1. Solve the undamped problem $\left(-\lambda_{r,0}\mathbf{M}+\mathbf{K}_e+\mathbf{K}_v^*(0)\right)\boldsymbol{\phi}_{r,0}=\mathbf{0}$ with $\boldsymbol{\phi}_{r,0}^{\mathrm{T}}\mathbf{M}\boldsymbol{\phi}_{r,0}=1$.
2. Initialize $j:=1$, define the convergence tolerance *Tol* and the maximum number of iterations $j_{\max}$.
3. Repeat
   4. Compute the real eigenfrequency $\omega_{r,j-1}$.
   5. Compute $\Delta\mathbf{K}_{r,j-1}^*=\mathbf{K}_v^*(\omega_{r,j-1})-\mathbf{K}_v^*(0)$.
   6. Compute $\Delta\lambda_{r,j-1}^*:=\boldsymbol{\phi}_{r,0}^{\mathrm{T}}\,\Delta\mathbf{K}_{r,j-1}^*\,\boldsymbol{\phi}_{r,0}$.
   7. Compute $\mathbf{f}_{r,j}^*:=-(-\Delta\lambda_{r,j-1}^*\mathbf{M}+\Delta\mathbf{K}_{r,j-1}^*)\boldsymbol{\phi}_{r,0}$.
   8. Compute $\mathbf{G}_{r,j}^*:=-\lambda_{r,0}\mathbf{M}+\mathbf{K}_e+\mathbf{K}_v^*(\omega_{r,j-1})$.
   9. Find the k position of the element with largest absolute value in $\boldsymbol{\phi}_{r,0}$ vector.
   10. Construct $\bar{\mathbf{G}}_{r,j}^*$ by zeroing out the k row and column of $\mathbf{G}_{r,j}^*$ and setting the k diagonal element to 1.
   11. Construct $\bar{\mathbf{f}}_{r,j}^*$ by zeroing out the kth element of $\mathbf{f}_{r,j}^*$.
   12. Solve $\mathbf{v}_{r,j}^*$ from the linear equation system $\bar{\mathbf{G}}_{r,j}^*\mathbf{v}_{r,j}^*=\bar{\mathbf{f}}_{r,j}^*$.
   13. Compute $c_{r,j}^*:=-\boldsymbol{\phi}_{r,0}^{\mathrm{T}}\mathbf{M}\mathbf{v}_{r,j}^*$.
   14. Compute $\boldsymbol{\phi}_{r,j}^*:=\boldsymbol{\phi}_{r,0}+\left(\mathbf{v}_{r,j}^*+c_{r,j}^*\boldsymbol{\phi}_{r,0}\right)$.
   15. Normalize $\boldsymbol{\phi}_{r,j}^*:=\dfrac{\boldsymbol{\phi}_{r,j}^*}{\sqrt{\boldsymbol{\phi}_{r,j}^{\mathrm{T}}\mathbf{M}\boldsymbol{\phi}_{r,j}^*}}$.
   16. Compute $\lambda_{r,j}^*:=\boldsymbol{\phi}_{r,j}^{*\mathrm{T}}\mathbf{K}^*(\omega_{r,j-1})\boldsymbol{\phi}_{r,j}^*$.
   17. Compute the error $\kappa_{r,j}$ and increase $j:=j+1$.

Until $\kappa_{r,j}\leqslant Tol$ or $j>j_{\max}$.

References

[1] D.I.G. Jones, *Handbook of Viscoelastic Vibration Damping*, John Wiley, Chichester, 2001.
[2] C.T. Sun, Y.P. Lu, *Vibration Damping of Structural Elements*, Prentice-Hall, New Jersey, 1995.
[3] A.D. Nashif, D.I.G. Jones, J.P. Henderson, *Vibration Damping*, Wiley, New York, 1985.

[4] N.O. Myklestad, The concept of complex damping, *Journal of Applied Mechanics* 19 (1952) 284–288.
[5] R.E.D. Bishop, The treatment of damping forces in vibrating theory, *Journal of the Royal Aeronautical Society* 59 (1955) 738–742.
[6] I.M. Ward, D.W. Hadley, *An Introduction to the Mechanical Properties of Polymers*, Wiley, Chichester, 1993.
[7] S.W. Park, Analytical modelling of viscoelastic dampers for structural and vibration control, *International Journal of Solids and Structures* 38 (44–45) (2001) 8065–8092.
[8] S. Adhikari, Damping models for structural vibration, Ph.D. Thesis, Cambridge University, 2000.
[9] T.J.R. Hughes, *The Finite Element Method: Linear Static and Dynamic Finite Element Analysis*, Dover Publishers, New York, 2000.
[10] K.J. Bathe, *Finite Element Procedures*, Prentice-Hall, New Jersey, 1996.
[11] D.J. Ewins, *Modal Testing*, 2nd ed., Research Studies Press, Baldock, 2000.
[12] C. Lanczos, An iteration method for the solution of the eigenvalue problem of linear differential and integral operators, *Journal on Research of the National Bureau of Standards* 45 (4) (1950) 255–282.
[13] W.E. Arnoldi, The principle of minimized iterations in the solution of the matrix eigenvalue problem, *Quarterly of Applied Mathematics* 9 (1951) 17–29.
[14] A.Y.T. Leung, Subspace iterations for complex symmetric eigenproblems, *Journal of Sound and Vibration* 184 (4) (1995) 627–637.
[15] C.D. Johnson, D.A. Kienholtz, L.C. Rogers, Finite element prediction of damping in beams with constrained viscoelastic layers, *Shock and Vibration Bulletin* 51 (1) (1981) 71–81.
[16] M.L. Soni, Finite element analysis of viscoelastically damped sandwich structures, *Shock and Vibration Bulletin* 51 (2) (1981) 97–108.
[17] C.D. Johnson, D.A. Kienholtz, Finite element prediction of damping in structures with constrained viscoelastic layers, *American Institute of Aeronautics and Astronautics Journal* 20 (9) (1982) 1284–1290.
[18] M.F. Kuesener, M.L. Drake, Damped structure design using finite element analysis, *Shock and Vibration Bulletin* 52 (1982) 1–12.
[19] D.V. Murthy, R.T. Haftka, Derivatives of eigenvalues and eigenvectors of a general complex matrix, *International Journal for Numerical Methods in Engineering* 26 (9) (1988) 293–311.
[20] F. Chatein, *Eigenvalues of Matrices*, John Wiley, New York, 1993.
[21] R.N. Nelson, Simplified calculation of eigenvector derivatives, *American Institute of Aeronautics and Astronautics Journal* 14 (9) (1976) 1201–1205.
[22] R.L. Fox, M.P. Kapoor, Rates of change of eigenvalues and eigenvectors, *American Institute of Aeronautics and Astronautics Journal* 6 (12) (1968) 2426–2429.
[23] B.P. Wang, Improved approximate methods for computing eigenvector derivatives in structural dynamics, *American Institute of Aeronautics and Astronautics Journal* 29 (6) (1991) 1018–1020.
[24] O. Zhang, A. Zerva, Iterative method for calculating derivatives of eigenvectors, *American Institute of Aeronautics and Astronautics Journal* 34 (5) (1996) 1088–1090.
[25] Using MATLAB Version 6, The MathWorks Inc., Natick, USA, 2001.
[26] D.C. Sorensen, Implicit Application of Polynomial Filters in a *k*-step Arnoldi Method, *SIAM Journal on Matrix Analysis and Applications* 13 (1992) 357–385.
[27] R.B. Lehoucq, D.C. Sorensen, C. Yang, *Arpack User's Guide: Solution of Large-Scale Eigenvalue Problems with Implicitly Restarted Arnoldi Methods*, SIAM, 1998. www.caam.rice.edu/software/ARPACK.
[28] R.L. Bagley, P. Torvik, A theoretical basis for the application of fractional calculus to viscoelasticity, *Journal of Rheology* 27 (3) (1983) 201–210.